

# Self-healing Restoration of Smart Microgrids in Islanded Mode of Operation

M. ZakiEl-Sharafy and H.E. Farag<sup>(✉)</sup>

Electrical Engineering and Computer Science, Lassonde School of Engineering,  
York University, Toronto, ON, Canada  
Eng.mzaki@hotmail.com, hefarag@cse.yorku.ca

**Abstract.** This paper proposes a new algorithm for optimum self-healing restoration of a smartmicrogrid operating in islanded mode of operation. The objective of the proposed algorithm is to optimize the topological structure of the islanded microgrid system (IMG) via: (1) maximizing the served load after the fault isolation; and (2) minimizing the switching operation costs. The proposed algorithm takes into consideration the system operational constraints in all operating conditions. The new algorithm accounts for droop controlled IMG special operational characteristics. The problem is formulated as a multi-objective optimization problem and solved using Ant Colony Optimization Algorithm. The proposed algorithm has been implemented in MATLAB environment and several case studies have been carried to test its effectiveness.

**Keywords:** Ant colony optimization algorithm · Islanded microgrid · Droop control · Power system restoration

## 1 Introduction

One of the most problems in the self-healing of the distribution system is the service restoration for a faulted area. When a fault takes place in distribution systems it affects the system reliability and the customer's satisfaction. As such to ensure a maximum reduction in the system reliability, the faulted area must be detected and isolated [1]. After the fault isolation, the Distribution Network Operator (DNO) reconfigures the distribution network to restore the outage (i.e. system restoration process) [2]. The main objective of the system restoration is to restore the out of service loads by transferring the power to them through alternative paths with minimum losses or to transfer these loads to other feeders. Due to delays in the outage processing and the required time for service crews, an outage time from minutes to several hours might be yielded [2]. This slow response in service restoration of conventional distribution networks remarkably affects the system reliability.

Nowadays, driven by technical, environmental and economical benefits, distribution networks are currently undergoing a profound paradigm shift towards active networks. Such networks are characterized by multidirectional power and information flow due to the integration of high penetration levels of distributed generation (DG) accompanied with advanced metering, communication and control technologies. The integration of DG units and other emerging components can have an impact on the

practices used in distribution systems. Therefore, various operational strategies are expected to face numerous challenges. With the high degree of complexities that is accompanied with the transformation of distribution networks, DNO might no longer be able to detect and isolate faults and/or restore the outage loads using the human operator's experimental rules. This in turn necessitates the need for implementing automated self-healing mechanisms in active distribution networks. There are many artificial intelligence methods that have been proposed in the literature to restore radial distribution systems [3–10].

The widespread implementation of DG units in distribution systems makes them capable of supplying all or most of their local power demands; which initiated the concept of microgrids. Microgrids are localized grids that are typically implemented in local areas (e.g. cities, towns, or villages) and capable of disconnecting from the traditional power grid to operate in island (i.e. able to operate in grid-connected and off-grid modes) [11, 12]. Because they are able to continue operating while the main grid is down, microgrids help mitigate grid disturbances to strengthen the grid resilience and customers' reliability [13, 14]. Further, under the smart grid paradigm, microgrids would be able to facilitate seamless integration for high penetration and wide variety of DGs, energy storage technologies and demand response [15, 16]. Interestingly, the concept of microgrids in energy sector is also interrelated to the recent vision of smart cities. Where, the development and implementation of "smart" microgrids is a key component in enhancing the livability, workability and sustainability, which are identified as the pillars of smart cities. For these reasons, microgrids can be identified as the building blocks of both smart power grids and cities.

Given the special control features and operational characteristics of islanded microgrids (IMG), the state-of-the-art self-healing restoration of distribution networks should be adopted to take IMG deployment into consideration. Up to the authors' knowledge, there is no previous work that addressed the problem of self-healing restoration in IMG. In this work, a new algorithm for self-healing restoration of IMG is proposed. Appropriate power flow models for DGs have been incorporated in the optimization problem to provide proper representation for microgrid components during islanded mode of operation. Ant Colony optimization has been utilized to solve the problem and several case studies have been conducted in order to validate the proposed IMG restoration algorithm.

## 2 Operation Mechanism of Islanded Microgrids

The majority of DG units forming microgrids are interfaced via dc-ac power electronic inverter systems. In islanded mode, droop control that enables active and reactive power sharing through the introduction of droop characteristics to the output voltage frequency and magnitude of dispatchable DG units is usually applied. In this section, a review for droop-based control scheme in IMG is presented.

## 2.1 Transmission Line Power Transfer Theory

The active and reactive power transfer in transmission lines is based on the operation characteristics of synchronous generators, where it depends on the voltage and the phase angle at both sending and receiving bus sides. The active power and reactive power flowing into the transmission line at the sending end can be given as follows:

$$S_i = P_i + jQ_i = u_i I^* = u_i \left[ \frac{u_i - u_j e^{-j\gamma}}{jX} \right]^* \quad (1)$$

$$P_i = \frac{u_i u_j}{X} \sin \gamma^* \quad (2)$$

$$Q_i = \frac{u_i (u_i - u_j \cos \gamma)}{X} \quad (3)$$

where;  $P_i$  is the active power at line  $i$ ,  $Q_i$  is the reactive power at line  $i$ ,  $S_i$  is the total complex power at line  $i$ ,  $u_i$  is the voltage at sending side,  $u_j$  is the voltage at receiving side,  $I$  is the current flow in the line,  $\gamma$  is the power angle, and  $X$  is the line inductance. In transmission lines, the power angle is very small, therefore it can be assumed that  $\sin \gamma = \gamma$  and  $\cos \gamma = 1$ . Accordingly, one can observe that the active power is strongly dependent on the power angle, while the reactive power is strongly dependent on the voltage of the sending and receiving ends. Therefore the frequency droop can regulate the active power and the voltage droop can regulate the reactive power. From the above discussion, the inverters in IMG are controlled to imitate the behaviors of synchronous machines by applying the following droop equations:

$$F - F_0 = -K_p (P - P_0) \quad (4)$$

$$u - u_0 = -K_q (Q - Q_0) \quad (5)$$

where,  $F$  is the system Frequency,  $u$  is the voltage magnitude,  $F_0$  is the nominal system frequency,  $u_0$  is the nominal voltage magnitude,  $P$  is the inverter output of active power,  $Q$  is the inverter output of reactive power,  $P_0$  is the momentary set point for the active power of the inverter,  $Q_0$  is the momentary set point for the reactive power of the inverter,  $K_p$  is the frequency droop coefficient, and  $K_q$  is the voltage droop coefficient.

## 2.2 Voltage and Frequency Control

Figure 1(a, b) shows the power sharing of two inverters based on droop control. Let's assume that the frequency droop coefficients of the two inverters are  $k_{p1}$  and  $k_{p2}$ , and the output active power of the two inverters are  $P_{10}$  and  $P_{20}$  at the nominal frequency of the grid  $f_0$ , respectively. When the load increases, the two inverters change their output power and the system frequency is changed from its nominal frequency to  $f_1$ . Such change in active power can be formulated mathematically as follows:

$$\Delta P_1 = P_{11} - P_{10} = -\frac{1}{K_{p1}}(f_1 - f_0) \tag{6}$$

$$\Delta P_2 = P_{21} - P_{20} = -\frac{1}{K_{p2}}(f_1 - f_0) \tag{7}$$

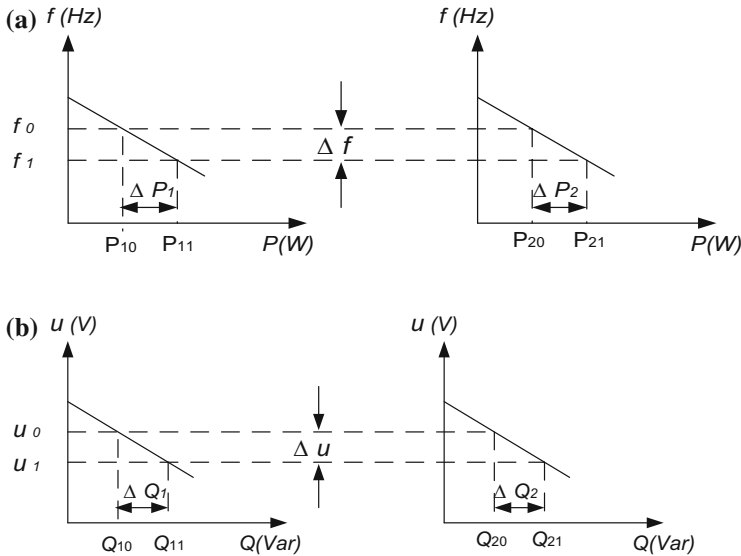


**Fig. 1.** (a): Power sharing in droop control: ( $P$ - $f$ ) characteristics (b): Power sharing in droop control: ( $Q$ - $U$ ) characteristics

Similar to (6) and (7), the two inverters share the reactive power demand. As shown in Fig. 1, the active and reactive power sharing is mainly governed by the static droop coefficients of active and reactive power, where

$$\frac{\Delta P_1}{\Delta P_2} = \frac{k_{p2}}{k_{p1}} \tag{8}$$

$$\frac{\Delta Q_1}{\Delta Q_2} = \frac{k_{q2}}{k_{q1}} \tag{9}$$

Equations (8) and (9) are used as virtual communication mediums among the inverters in order to represent the active and reactive power sharing between the DGs. For  $n$  droop-controlled DG units, (10) and (11) below are met

$$\Delta P_1.k_{p1} = \Delta P_2.k_{p2} = \dots = \Delta P_n.k_{pn} \tag{10}$$

$$\Delta Q_1.k_{q1} = \Delta Q_2.k_{q2} = \dots = \Delta Q_n.k_{qn} \tag{11}$$

Here it is noteworthy that the aforementioned analysis is under the strong assumption that the DG units are highly inductive due to the coupling inductor used in the DG interface. If the system is resistive, however, the equation will be given by (P-f) and (Q-U) instead.

### 3 Problem Formulation of Service Restoration in IMG

The problem of self-healing restoration in IMG is formulated in this section as an optimization problem as follows:

#### 3.1 Objective Functions

The main objective functions in the restoration are maximizing the restored load (12) and minimizing the number of switching operations (13).

$$\max \sum_{X \in D} L_X \cdot j_X \quad (12)$$

$$\min \sum_{X \in D} SW_X \quad (13)$$

where;

$L_X$ : The load at bus no. X,  $j_X$ : The binary decision whether the load at bus X is restored ( $j_X = 1$ : restored,  $j_X = 0$ : not restored),  $D$ : The set of all de-energized loads,  $SW_X$ : Representation of the switching operation in bus X ( $X_X = 1$ : the switch state is changed,  $X_X = 0$ : no change occurs in the switch state).

#### 3.2 Constraints of the IMG Service Restoration Problem

In the self-healing restoration process for the IMG system, the constraints can be represented as follow:

- (1) **The Voltage level:** for every bus load at the distribution system the voltage level must be maintained to be within range of  $\pm 5\%$  from the p.u. value.

$$u_{min} \leq u_X \leq u_{max} \quad (14)$$

where;  $u_{min}$  And  $u_{max}$ : Minimum and maximum voltage levels at bus X respectively (95–105 %),  $u_X$ : The voltage level at bus X

- (2) **Power Balance Equations:** The Active and reactive power balance between supply and demand.

$$P_i(|u_i|, |u_j|, \partial_i, \partial_j, w) - PG_i(w) + PL_i(|u_i|, w) \cong 0 \quad (15)$$

where;  $PG_i$ : The total active power from supply,  $PL_i$ : The total active power demanded at the load,  $P_i$ : The total active power at bus  $i$ ,  $\partial_i$ : Phase angle at bus  $i$ ,  $\partial_j$ : Phase angle at bus  $j$ .

$$Q_i(|u_i|, |u_j|, \partial_i, \partial_j, w) - QG_i(|u_i|) + QL_i(|u_i|, w) \cong 0 \quad (16)$$

where;  $QG_i$ : The total Reactive power from supply,  $QL_i$ : The total Reactive power demanded at the load,  $Q_i$ : The total Reactive power at bus  $i$

(3) **Droop-controlled DG units constrains:** The capacity of DG units and the limits of the droop parameters ( $Kp$ ,  $Kq$ ,  $w^*$ ,  $u^*$ )

$$P_{Gi} \leq S_{Gi,max} \quad (17)$$

$$Q_{Gi} \leq \sqrt{(S_{Gi,max} - (P_{Gi})^2)} \quad (18)$$

$$0 \leq Kp_i \quad (19)$$

$$0 \leq Kq_i \quad (20)$$

$$59.5 \text{ HZ} \leq w^*_i \leq 60.5 \text{ HZ}(w_{max}) \quad (21)$$

where;  $P_{Gi}$ : Generated active power from DG  $i$ ,  $Q_{Gi}$ : Generated Reactive power from DG  $i$ ,  $S_{Gi,max}$ : MVA rating of DG  $i$ ,  $Kp$  and  $Kq$  are the droop control setting for the DG  $i$ ,  $w^*_i$  is the requested frequency for the DG to reach it's sharing level (same as the system frequency), finally the voltage level for the DG bus is the same as (14)

(4) **Feeder line current limits** should be also taken into consideration as follows:

$$I_{min} \leq I_j \leq I_{max} \quad (22)$$

where;  $I_{min}$  and  $I_{max}$  are the minimum and maximum current level of the line respectively,  $I_j$  is the current level of line  $j$ .

## 4 IMG Self-healing Restoration Based on ACO

The ant colony optimization is a stochastic population based heuristic algorithm which is equivalent to the behavior of the ant or bee in there colony in the real life [17]. ACO is widely used in solving the problem of self-healing restoration in active distribution networks. ACO can also be used to solve the problem of self-healing restoration in IMG, where the outage buses findits own feeder bus as follows [7]:

$$P_{ij} = \frac{(\tau_{ij})^\alpha (\eta_{ij})^\beta}{\sum_{s \in allowed k} (\tau_{is})^\alpha (\eta_{is})^\beta} \tag{23}$$

where;  $P_{ij}$ : The probability of the ant to move from point  $i$  to  $j$ ,  $\tau_{ij}$ : The quantity of remnant pheromone on the trail from  $i$  to  $j$ ,  $\eta_{ij}$ : The desirability of the trail which is  $1/distance$ ,  $\beta$ : The parameters that control the relative importance of the trail pheromone versus the desirability of the trail. When all ants have completed a tour, the pheromone trails are globally updated using the global pheromone-updating rule (24). The aim of the pheromone update is to increase the pheromone values associated with good or promising solutions, and to decrease those that are associated with bad ones based on (25).

$$\tau_{ij} = (1 - \rho)\tau_{ij} + \Delta\tau_{ij} \tag{24}$$

where,  $\rho$  is the evaporation of trail pheromone between  $i$  and  $j$  and  $\Delta\tau_{ij}$  is the pheromone left on trail  $ij$  by current optimal solution given as follows:

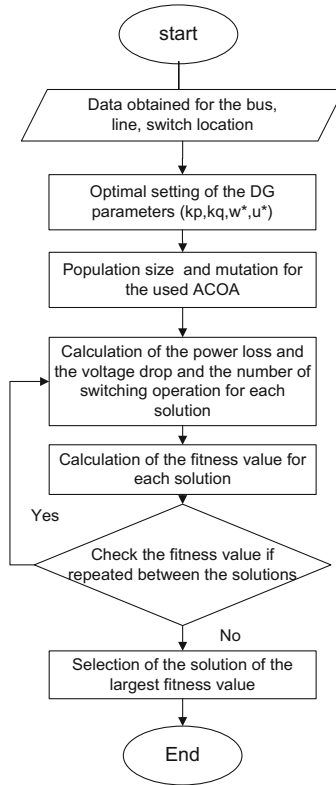


Fig. 2. Flowchart for the proposed self-healing restoration process in IMG

$$\Delta\tau_{ij} = Q/L_S \tag{25}$$

where,  $Q$  is a constant and  $L_S$  is the tour length of the ant  $s$  to the whole trip. The optimum solution is obtained; after a number of iterations, comparing the probability of each path with each other, and by choosing the one with the highest probability. Where the total self-healing restoration process can be represented as shown in Fig. 2.

### 5 Simulation and Results

The 33-bus distribution test system shown in Fig. 3 has been used in this work to test the effectiveness of the proposed self-healing restoration algorithm in IMGs. As shown in the figure, four dispatchable DGs are installed. According to the droop settings of DG units, two base case studies have been carried out during the normal operation of IMG. In the first case study, a capacity-based power sharing of DG units has been implemented. In this case, the static droop coefficients of the DG units are calculated in proportion to the capacities of DG units. Table 1 shows the droop settings in the first case study. In the second case study, the droop settings of the DG units are optimally selected to minimize the total system losses of the IMG. Table 2 shows the droop settings for optimal power sharing during the normal operation of the IMG (i.e. no fault). Table 3 presents the total system losses and the minimum voltage level in the two case studies. Figure 4 shows the voltage magnitude in per unit for the system buses in the base case studies. The results

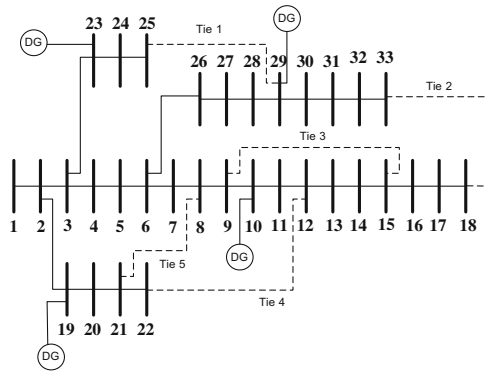


**Fig. 3.** The 33 IEEE-bus system represented as a microgrid in islanded mode of operation

**Table 1.** Droop settings for case study #1: capacity-based sharing

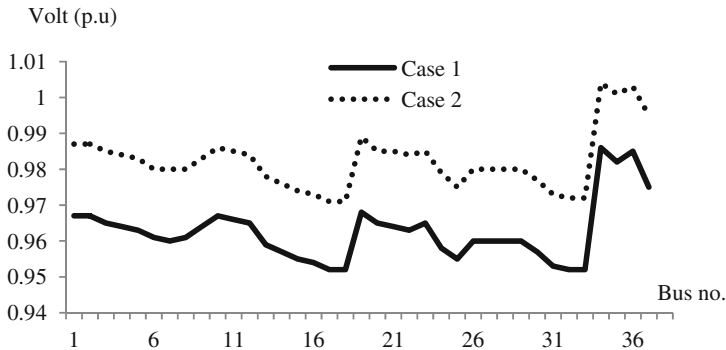
DG#	Bus location	Rating MVA	$k_p$	$k_q$	$u^*$ (p.u.)	$w^*$ (p.u.)
1	10	2	0.0027/2	0.05/2	1.01	1
2	29	2	0.0027/2	0.05/2	1.01	1
3	23	2	0.0027/2	0.05/2	1.01	1
4	19	2	0.0027/2	0.05/2	1.01	1

**Table 2.** Droop settings for case study #2: optimal power sharing

DG#	Bus location	Rating MVA	$k_p$	$k_q$	$u^*$ (p.u.)	$w^*$ (p.u.)
1	10	2	0.0014/2	0.025/2	0.9856	1.0044
2	29	2	0.0014/2	0.025/2	1.01	1.0001
3	23	2	0.0019/2	0.032/2	0.9895	1.0073
4	19	2	0.0016/2	0.029/2	0.9956	1.0067

**Table 3.** Steady state system losses and voltage in normal operation

Steady state	Case study 1	Case study 2
Total system losses	0.111MVA	0.106MVA
Min. voltage level	0.951 p.u.	0.951 p.u.

**Fig. 4.** Voltage profile of the islanded microgrid during normal operation

show that optimal power sharing of droop-controlled DG units reduces the system losses and enhances the voltage profile significantly.

The above case studies have been repeated in the self-healing restoration process. It is assumed that a fault occurs between bus 10 and bus 11, where the loads from bus 11 to the downstream is out of service and need to be restored. According to the topology of the studied system, it can be noticed that Tie 2, 3 and 4 are only the candidate paths in order to restore the faulted area, where only one switching operation of them can be used to satisfy the restoration problem. However, when the losses minimization is taken into account, there might be several required switching actions. To determine the optimal switching actions for maximizing the load restoration, minimizing the system losses, minimizing the switching operation and satisfying the operation constraints, the proposed ACO needs to be executed.

After the occurrence of the faulted area, the restoration process is carried by the ACO to choose from different switching actions to restore the faulted area, which can

help the microgrid operator to take appropriate decision. The challenge in the self-healing restoration is thus prevailing in taking an optimal decision that is a trade-off between the minimum losses and the number of switching operations, where as the number of switching operation increases the total cost of the restoration process is also increased. In this work a limit of 3 switching operations has been assumed in order to study the impacts of the number of switching operations on the solution of the optimization problem. Here it is noteworthy that in the 2<sup>nd</sup> case study, the restoration process is also achieved by using ACO while in this case the new droop setting for the DGs that can optimize the system operation is applied (i.e. For each candidate solution (i.e. configuration), a nonlinear optimization problem is solved to determine the droop settings of DG units).

Table 4 shows the results of the proposed self-healing restoration process in the two case studies with different switching operation. Figures 5 and 6 show the total system losses and the voltage profile in the two case studies with different switching operation. As shown in the results, the optimal power sharing among the droop-controlled DG

**Table 4.** Results of the proposed self-healing restoration process in IMG

Comparison points		1 Switching Operations	2 Switching Operations	3 Switching Operations
Total system losses	1 <sup>st</sup> Case	0.1139 MVA	0.1139 MVA	0.11253 MVA
	2 <sup>nd</sup> Case	0.109713 MVA	0.1089 MVA	0.1089 MVA
Min. voltage level	1 <sup>st</sup> Case	0.951 p.u.	0.949 p.u.	0.948 p.u.
	2 <sup>nd</sup> Case	0.9708 p.u.	0.9696 p.u.	0.9675 p.u.
Switching action	1 <sup>st</sup> Case	Close Tie 3	Close Tie 3, Open Tie between bus 3 and 23	Close Tie 3 & Tie 1, Open Tie between bus 28 and 29
	2 <sup>nd</sup> Case	Close Tie 3	Close Tie 3, Open Tie between bus 3 and 23	Close Tie 3 & Tie 1, Open Tie between bus 26 and 27

units in IMG will enhance the system losses. Further, as depicted in the results, the voltage profile for the buses has been significantly improved.

As shown in Fig. 5, the minimum voltage occurred in all switching scenarios in case study 2 is within the range of the voltage constrains. However, in some switching operation scenarios, in the 1<sup>st</sup> case study, the voltage magnitude violated its lower bound, which is a critical state for the total system. The DNO can use the obtained results to compromise between the total losses and the cost of the switching operation.

A key factor that needs to be taken into account in the self-healing restoration process is the time of execution. Where, it is critical to restore the faulted loads as quick as possible. In the proposed algorithm, the number of iterations that has been taken in this process to restore the loads was found to be 9 iterations for the ACO to take the

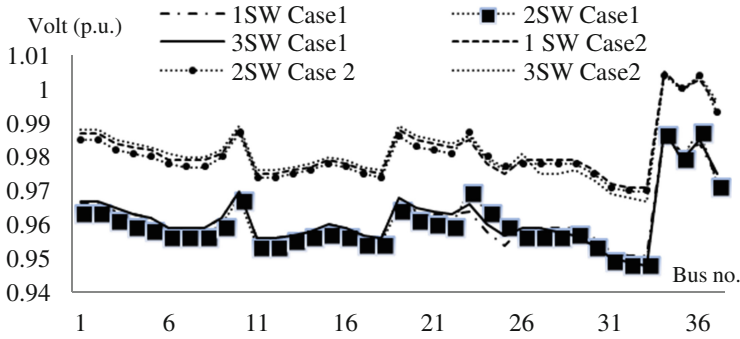


Fig. 5. Voltage profile for all restoration scenarios

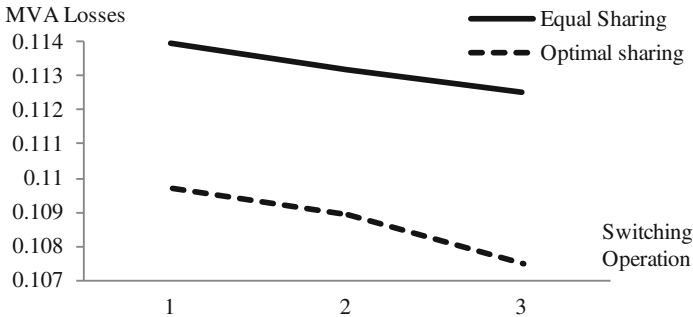


Fig. 6. Pareto optimal front for the total system losses

decision in all possible switching actions, and 3 to 12 iterations for the power flow for every nominated configuration for the system. The processor used to conduct the simulation was Intel® Core™2 Duo CPU P8700 @ 2.53 GHz with system type of 32-bit operating system and the installed memory was 4.00 GB. Where at this specs the duration time taken from the ACO to propose the suitable configuration was 115.25 s. The obtained execution time of the proposed self-healing restoration process is acceptable to the microgrid operator in order to do the switching actions in the system.

## 6 Conclusion

In this paper a new algorithm has been proposed for the optimum self-healing restoration of a microgrid operating in islanded mode. The proposed algorithm aims to maximize the capacity of the restored load. In addition, the proposed algorithm aims to choose the optimum configuration that compromises the trade-off of between two objective functions; namely number of switching and the system losses. Two different operational control schemes (without and with optimal power sharing) have been implemented in the proposed algorithm to account for the impacts of the selection of

the droop parameters on the enhancement of the IMG restoration process. The problem has been formulated as a mixed integer nonlinear optimization. The ACO has been utilized to solve the optimization problem. To handle the trade-off between the two objectives, the Pareto optimal configuration for each operational scenario has been determined. The results show that optimizing the IMG power sharing would enhance its restoration process.

## References

1. Faria, L., Silva, A., Vale, Z., Marques, A.: Training control centers' operators in incident diagnosis and power restoration using intelligent tutoring systems. *IEEE Trans. Learn. Technol.* **2**(2), 135–147 (2009)
2. Oualmakran, Y., Melendez, J., Herraiz, S.: Opportunities and challenges for smart power restoration and reconfiguration smart decisions with smart grids. In: 2011 11th International Conference on Electrical Power Quality and Utilisation (EPQU), pp. 1–6 (2011)
3. Prakash, M., Pradhan, S., Roy, S.: Soft computing techniques for fault detection in power distribution systems: a review. In: 2014 International Conference on Green Computing Communication and Electrical Engineering (ICGCCEE), pp. 1–6 (2014)
4. Sujil, A., Agrwal, S.K., Kumar, R.: Centralized multi-agent self-healing power system with super conducting fault current limiter. In: 2013 IEEE Conference on Information & Communication Technologies (ICT), pp. 622–627 (2013)
5. Zidan, A., El-Saadany, E.F., El Chaar, L.: A cooperative agent-based architecture for self-healing distributed power systems. In: IEEE Conference on Innovations in Information Technology (IIT), pp. 100–105 (2011)
6. Gonzalez, R.O., Gonzalez, G.G., Escobar, J., Barazarte, R.Y.: Applications of Petri nets in electric power systems. In: Central America and Panama Convention (CONCAPAN XXXIV). IEEE, pp. 1–6 (2014)
7. Abd El-Hamed, M.Z., El-Khattam, W., El-Sharkawy, R.: Self-healing restoration of a distribution system using hybrid fuzzy control/ant-colony optimization algorithm. In: 2013 3rd International Conference on Electric Power and Energy Conversion Systems (EPECS), pp. 1–6 (2013)
8. Karn, R., Kumar, Y., Agnihotrim, G.: Development of ACO algorithm for service restoration in distribution system. *Int. J. Emerging Technol.* **2**(1), 71–77 (2011)
9. Mustafa, M., El-Khattam, W., Galal, Y.: A novel fuzzy cause-and-effect-networks based methodology for a distribution system's fault diagnosis. In: 2013 3rd International Conference on Electric Power and Energy Conversion Systems (EPECS), pp. 1–6 (2013)
10. Malakhov, A., Kopyriulin, P., Petrovski, S., Petrovski, A.: Adaptation of smart grid technologies. In: 2012 IEEE International Conference on Fuzzy Systems (FUZZ-IEEE), pp. 1–6 (2012)
11. Cheng, S., Junyong, L., Yang, J., Ni, Y., Xiang, Y., Zhu, X., Tian, H.: Optimal coordinated operation for microgrid with hybrid energy storage and diesel generator. In: 2014 International Conference on Power System Technology (POWERCON), pp. 3207–3212 (2014)
12. Jouybari-Moghaddam, H., Hosseinian, S.H., Vahidi, B., Rad, M.G.: Smart control mode selection for proper operation of synchronous distributed generators. In: 2012 2nd Iranian Conference on Smart Grids (ICSG), pp. 1–4 (2012)

13. Ashabani, S.M., Mohamed, Y.A.-R.I.: New family of microgrid control and management strategies in smart distribution grids—analysis, comparison and testing. *IEEE Trans. Power Syst.* **29**, 2257–2269 (2014)
14. Etemadi, A.H., Davison, E.J., Iravani, R.: A generalized decentralized robust control of islanded microgrids. *IEEE Trans. Power Syst.* **29**(6), 3102–3113 (2014)
15. Lee, D.-L., Wang, L.: Small signal stability analysis of an autonomous hybrid renewable energy power generation/energy storage system Part I: time domain simulation. *IEEE Trans. Energy Convers.* **23**(1), 311–320 (2008)
16. Miao, Z., Domijan, A., Fan, L.: Investigation of microgrids with both inverter interfaced and direct AC connected distributed energy resources. *IEEE Trans. Power Delivery* **26**(3), 1634–1642 (2011)
17. Hlaing, Z.C.S.S., Khine, M.A.: Solving traveling salesman problem by using improved ant colony optimization algorithm. *Int. J. Inf. Educ. Technol.* **1**(5), 81–87 (2011)